A Theoretical Analysis of the Effects of Tumor-Treating Electric Fields on Single Cells

Xing Li,[1]* **Fan Yang**,[1] **Bing Gao**,[1] **Xiao Yu**,[1] **and Boris Rubinsky**[2]

[1]*State Key Laboratory of Power Transmission Equipment & System Security and New Technology, School of Electrical Engineering, Chongqing University, Chongqing, China*

[2]*Department of Mechanical Engineering, University of California Berkeley, Berkeley, California*

Tumor-treating fields (TTFields) are low-intensity and intermediate-frequency alternating electric fields that have been found to inhibit tumor cell growth. While effective, the mechanism by which TTFields affect cell growth is not yet clearly understood. Although numerous mathematical studies on the effects of electromagnetic fields on single cells exist, the effect of TTFields on single cells have been analyzed less frequently. The goal of this study is to explore through a mathematical analysis the effects of TTFields on single cells, with particular emphasis on the thermal effect. We examine herein two single-cell models, a simplified spheroidal model and a simulation of a U-87 MG glioblastoma cell model obtained from microscopic images. A finite element method is used to analyze the electric field distribution, electromagnetic loss, and thermal field distribution. The results further prove that the electric field in the cytoplasm is too weak and its thermal damage can be excluded as a mechanism for cell death in TTFields. © 2020 Bioelectromagnetics Society.

Keywords: **tumor-treating fields; electric field distribution; electromagnetic loss; thermal effect; single-cell modeling**

INTRODUCTION

Tumor-treating fields (TTFields) are a variety of alternating electric fields with low-intensity (1–3 V/cm) and intermediate-frequency (100–300 kHz) that were first found by Kirson et al. [2004] to have the effect of inhibiting tumor cell growth. The effect has been found to be both safe and effective on several cell lines, including U-87 GM, B16F1, MDA-MB-23, and H1299 [Kirson et al., 2007; Pless et al., 2013]. Among these, clinical experiments on U-87 GM have already been carried out and achieved effective outcomes, and the Food and Drug Administration (FDA) has approved its application for treatment of recurring glioblastoma multiforme (GBM) after surgery and radiotherapy [Turner et al., 2014; Rehman et al., 2015]. On the basis of existing research results, relevant therapy systems have been developed by Novocure (Jersey, UK), which effectively prolonged the life of cancer patients [Mun et al., 2018].

However, although good results have been achieved both in vitro and in vivo, the biophysical mechanisms at play during exposure to TTFields are not yet fully understood. Thus far, these results have most commonly been attributed to the effect of the electric field on mitosis during cell division.

It has been suggested that TTFields in the cytoplasm can disrupt the polymerization of microtubules, resulting either in cell death or the slowing of cell growth [Gera et al., 2015]. This view notes that the microtubule dimer, which is the basic unit comprising the microtubule, has a large electric dipole moment that will tend to align parallel to the direction of an applied electric field. The torque imposed on the dimer will make it difficult to assemble microtubules and cause difficulties in spindle formation, culminating ultimately in failure of mitosis. Furthermore, in the telophase of mitosis, the electric field intensity in the cell is extremely non-uniform, and can result in dielectrophoretic (DEP) force [Piacentini et al., 2011]. The DEP force in the cleavage furrow is much

Grant sponsors: National Natural Science Foundation of China; grant number: 51777023; the National '111' Project of China; grant number: B08036.

Conflicts of interest: None.

*Correspondence to: Xing Li, State Key Laboratory of Power Transmission Equipment & System Security and New Technology, School of Electrical Engineering, Chongqing University, Chongqing 400044, China. E-mail: lixing@cqu.edu.cn

Received for review 8 July 2019; Accepted 24 May 2020

DOI:10.1002/bem.22274
Published online 00 Month 2020 in Wiley Online Library (wileyonlinelibrary.com).

stronger than elsewhere in the dividing cell and can drive macromolecules, such as the microtubule dimers and some organelles, to the cleavage furrow and may affect normal polymerization of microtubules. Although some morphological changes of the spindle have been detected via fluorescence microscopy [Giladi et al., 2015], they cannot be interpreted as direct evidence of the electric field destroying microtubule assembly via the torque and force mechanisms mentioned above. Some researchers further doubt whether the potential force and torque generated by the TTFields are sufficiently strong to exert a significant effect on the microtubule dimer [Wenger et al., 2018]. The thermal effect of TTFields, another potential driver of the observed clinical effects, has not been studied in previous studies, and is generally estimated to be insignificant due to the relatively low frequencies at play. Herein, we explore this notion, and to best understand the underlying mechanisms of the TTFields, we analyze the thermal effect at the single-cell level.

In theoretical analysis of electrical effects on the cell, traditionally, most works have focused on the cell trans-membrane voltage (TMV) calculation [Schwan, 1957; Kotnik and Miklavčič, 2000a]. For the bio-thermal effect studies of external electromagnetic fields, the source of the thermal effect is from electromagnetic loss, and thus most studies have focused on power dissipation, especially at the tissue level [Bottomley and Andrew, 1978]. Kotnik and Miklavčič [2000b] mathematically analyzed the conductive and dielectric power dissipation in cells exposed to alternating current (AC) electric fields based on the spherical cell model, but the irregular shape of real cells was not considered. To study whether the TTFields can cause significant thermal damage on single cells, more geometrically accurate cell models should be built and more comprehensive analysis of electromagnetic field effects on the single-cell exposed to the TTFields should be conducted.

In this paper, we employed a mathematical model to investigate the thermal and electromagnetic effects of TTFields on a single cell. We first improved the traditional spherical cell model by taking the nucleus into consideration, and then the potential and electric field distributions were derived theoretically by solving the Laplace equation. For the more complex situation reflected in reality, we used a microscopic image of a U-87 MG glioblastoma cell to determine the shape of the irregular cell model and develop a geometrically corresponding irregular cell model. On the basis of this model, the finite element method (FEM) was used to compute the electric field, electromagnetic loss, and temperature distribution. Finally, to address the thermal effect of TTFields, a conductive heat transfer model was used to calculate the temperature distribution in the cell. Furthermore, we imposed the electric field experimentally on a cell culture and measured the temperature change via an infrared camera. The results verified the correctness of the hypothesis that the TTFields produced no thermal damage to the cell, and that thermal damage can be excluded as a mechanism of cell death in TTFields.

MODEL AND METHOD

Regular Spherical Cell Model. Biological cells are found in various geometries, such as spheres, polyhedrons, spindles, cylinders, and so forth. A sphere yields the simplest approximation of cell shape and enables analytical calculation of the electric field distribution within the cell. The spherical cell model is thus the most classically employed model in biophysical analysis of the single cell. In order to theoretically derive and compare the results calculated from the traditional spherical cell model to the irregular model developed in this work, first the spherical model is developed while taking the nucleus into consideration, which was neglected in most previous models. This spherical cell model and geometrical parameters [Joshi et al., 2004] are shown in Figure 1.

Irregular Cell Model. In reality, only a small portion of biological cells are spherical or nearly spherical when they are in suspension, with most instead having various irregular shapes in vivo. Thus, the study results obtained from spherical cell models may be low in accuracy, and to improve the accuracy and evaluate the error between different cell models, more realistic irregular models should be established. Microscopic images of cells can provide some basic inspiration for geometrically irregular cell modeling.

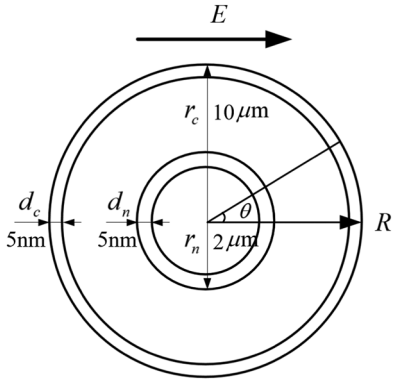

Fig. 1. Spherical cell model.

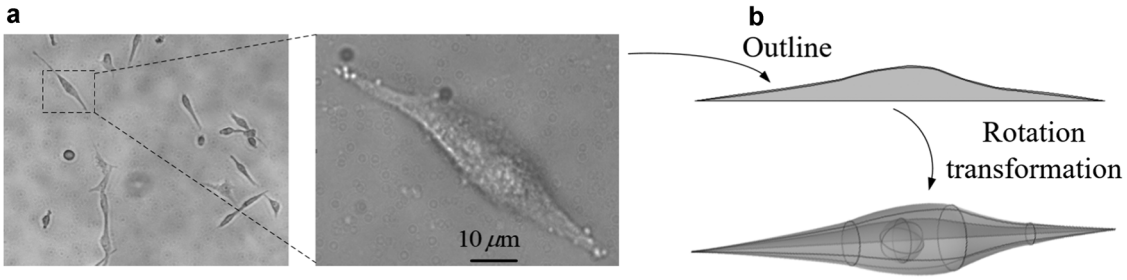

Fig. 2. The process of developing an irregular single-cell model of U-87 MG glioblastoma cell: (**A**) the microscopic image; (**B**) the model developed in COMSOL.

A U-87 cell is provided as an example, and its microscopic images are shown in Figure 2A. As depicted in the figure, the cell takes an elongated shape, which tapers as it extends in both directions, and the nucleus is not located in the middle of the cytoplasm. The size of the irregular cell is roughly 80-μm long and 20-μm wide. According to the outline of the cell images, we can develop an approximate geometrically irregular model by using a second-order Bezier curve and a rotation transformation as shown in Figure 2B.

We used cellular electrical parameters from the literature (Table 1) and treated the extracellular medium as physiological saline. Data in Table 1 are obtained at 35°C for frequencies that range from several kilohertz to several hundred kilohertz, permitting them to be regarded as frequency-independent [Kotnik and Miklavčič, 2000b]. For simplicity and comparison of different results, both the spherical and irregular cell models employ the same electrical parameters in this work.

Calculation of Physical Fields. From a physical point of view, to address the effects of TTFields, the intensity distribution of physical fields must be analyzed, including the distribution of the electric field intensity and temperature. Due to the fact that the frequencies of TTFields are from approximately 100 to 300 kHz, the wavelength is much longer than the size of cell, so the wave characteristic of the electric field can be ignored and the external electric field applied to the cell can be assumed homogeneous at every moment. In addition, the permittivity of the cell is in the β dispersion zone and the dispersion effect is negligible in the small range of frequency variation [Ponne and Bartels, 1995]. Furthermore, the permittivity and conductivity for frequencies range from several kilohertz to several hundred kilohertz, permitting them to be regarded as frequency-independent [Kotnik and Miklavčič, 2000b]. The inhomogeneity of the electrical parameters in each part of a cell is ignored in the following derivation and calculation.

The potential distribution in a cell exposed to an external electric field is determined from Laplace's equation,

$$\nabla^2 \phi = 0 \tag{1}$$

The boundary conditions between the different mediums are

TABLE 1. Electrical Parameters of the Cell

Parameter	Value	References
Conductivity of cell membrane	3×10^{-7} S/m	Gascoyne et al. [1993]
Conductivity of cytoplasm	0.3 S/m	Harris and Kell [1983]
Conductivity of nucleus membrane	5×10^{-7} S/m	Joshi et al. [2004]
Conductivity of nucleoplasm	0.2 S/m	Joshi et al. [2004]
Conductivity of extracellular medium	1.2 S/m	Sunderman [1945]
Permittivity of cell membrane	5 ε_0	Gascoyne et al. [1993]
Permittivity of cytoplasm	73 ε_0	Büchner et al. [1999]
Permittivity of nucleus membrane	136 ε_0	Joshi et al. [2004]
Permittivity of nucleoplasm	10 ε_0	Joshi et al. [2004]
Permittivity of extracellular medium	73 ε_0	Büchner et al. [1999]
Permittivity of the vacuum	$\varepsilon_0 = 8.854 \times 10^{-12}$ F/m	

$$\begin{cases} \phi_1 = \phi_2 \\ \sigma_1 \dfrac{\partial \phi_1}{\partial r} = \sigma_2 \dfrac{\partial \phi_2}{\partial r} \end{cases} \quad (2)$$

where ϕ is the electrical potential, σ is the local electrical conductivity in the cell, r is the radius direction in spherical coordinate system, and the subscripts 1 and 2 represent the two sides of the boundary.

For the spherical cell model illustrated in Figure 1, the boundary value problem of Equations (1)–(2) can be solved analytically with Legendre function [Joshi et al., 2004].

Hence, after obtaining the potential distribution, the electric field intensity can be derived by

$$E = -\nabla \phi \quad (3)$$

Addressing the thermal field calculation, due to the fact that the TTFields are sub-MHz, the dielectric power dissipation in the cell is negligible [Kotnik and Miklavčič, 2000b], and the conductive power dissipation caused by the friction of current carriers is the main component. According to electromagnetic theory, the conductive power dissipation density distribution p will be

$$p = \sigma E^2 \quad (4)$$

The whole electromagnetic power dissipation in the single cell can be calculated by the integral

$$P = \int_V \sigma E^2 \cdot dV \quad (5)$$

To address the thermal effect, the electromagnetic dissipation can be considered as the heat source, and the stationary temperature distribution of the cell can be derived from conductive heat transfer theory as

$$\begin{Bmatrix} \nabla^2 T + \dfrac{Q}{\lambda} = 0 \\ Q = p \end{Bmatrix} \quad (6)$$

where T is the temperature distribution, Q is the thermal power density, and λ is the thermal conductivity.

For the irregular cell model in an external electric field, the above mathematical formulas must be solved by numerical methods (COMSOL Multiphysics version 5.3; COMSOL, Stockholm, Sweden). The DC/AC module in the frequency domain of COMSOL was used to solve the electric field distribution problem. The mesh sizes for regular and irregular single cell models are 431,258 elements with 72,572 nodes and 984,209 elements with 165,072 nodes, respectively. The average size of each element is roughly 10^{-2} μm^3.

To obtain more accurate experimental data by simulation, a uniform external field was generated by two parallel electrodes on both sides of the cell, as shown in Figure 3. Simply, when calculating the thermal effect, ignoring the fluid properties of cytoplasm and extracellular medium, a thermal analysis was done using the COMSOL heat transfer module to model conductive heat transfer and the resulting temperature distribution within a biological cell.

In the practical application, the electric field for the GBM treatment is 2 V/cm, 200 kHz [Giladi et al., 2015]. Therefore, a certain voltage is applied on the electrodes in the model to generate an electric field typical of the in situ electric field of the Novocure medical device.

RESULTS

This section will show the results of the analysis of the physical fields. First, the spatial distributions of electric field, electromagnetic power dissipation, and temperature rise are described. Second, frequency-dependence of the electric field and thermal distribution was determined over 100 kHz to 1 MHz (at the same amplitude). The cell membrane is ignored in the thermal model because significant heating only occurs in the cytoplasm.

Spatial Distribution of Physical Fields. Figure 4 shows the calculated electric field intensity distributions in the two-cell models for the nominal device-generated

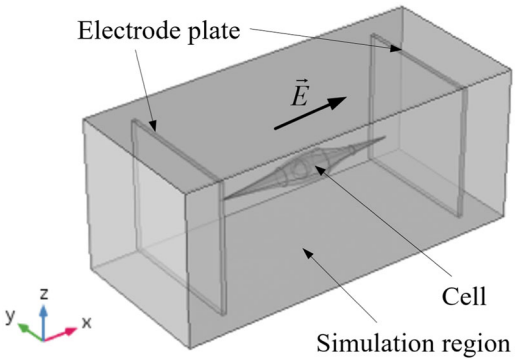

Fig. 3. Schematic of the irregular cell model in a uniform field.

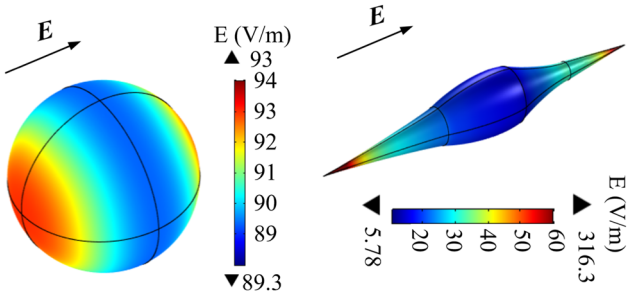

Fig. 4. The electric field intensity distributions.

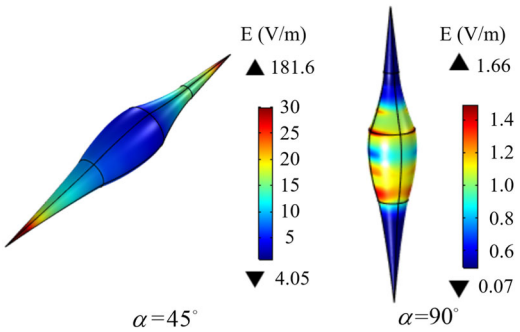

Fig. 6. The electric field intensity distributions in the irregular cell when the external electric field directions are varied.

electric field (2 V/cm at 200 kHz). Note the different scales, the equivalence of 1 and 100 V/m, and that very near the two tips the numerical calculation for the irregular model yields exceptionally high electric field values for a few voxels that can be ignored as unphysical consequences of the needle-like tip shape (similarly hereinafter).

Figure 4 indicates that the electric field distribution in the irregular cell is much more non-uniform than that in the spherical cell, and much stronger electric fields concentrate on the two ends of the cell.

Because the irregular cell model is not symmetrical, different directions of external electric fields must be considered. As illustrated in Figure 5, the angle between the electric field direction and the major axis of the irregular cell model is defined as α.

To investigate the effect of different external electric field directions, the irregular cell model is rotated by 45° and 90° and keeps all other simulation conditions unchanged. After simulation, the electric field intensity distributions in the irregular cell model are shown in Figure 6.

From the results of the electric field intensity distribution, it is easy to find that the electric field in the irregular cell varies greatly and is heavily dependent on the direction of electric field. When the electric field direction is parallel to the major axis of the cell, the electric field will be much stronger. Therefore, in the clinical application, applying electric fields in different directions can enhance the chance that the applied field will be approximately parallel to the axial direction of any particular tumor cell, and thereby may enhance the disruptive effect of electric fields on the cells.

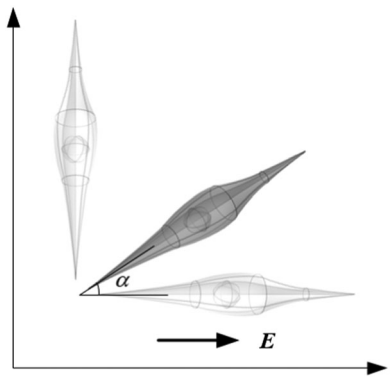

Fig. 5. Sketch of the angle between the electric field direction and the cell major axis.

After analyzing the electric field in the cell, thermal effects were studied using the model's electric field distribution. Thermal damage is one of the most important effects in biophysics, and is often used to kill tumors, mostly during tumor ablation. It is thus essential to study whether the TTFields produce a significant thermal effect. First, as the thermal source, electromagnetic power dissipation in the two single-cell models is calculated and the results are shown as Figure 7.

Figure 7 shows that in the spherical model (left), power density is nearly uniform in a narrow range near 1.2×10^3 W/m^3 over the entire volume. Maxima (red and upward triangle) occur at polar caps aligned with the field, but are only approximately 6% greater than minima at the equatorial region (blue and downward triangle). In sharp contrast, for the irregular model aligned with the field ($\alpha = 0°$), power density in the central bulge (blue) is significantly less (below 100 W/m^3, $\alpha = 0°$), somewhat lesser at $\alpha = 45°$, and near zero for $\alpha = 90°$. Power density in the tips varies even more sharply with orientation angle as it ranges from extremes many thousands of times greater than for the sphere over a substantial tip region for $\alpha = 0°$, to somewhat lower maxima for $\alpha = 45°$, and to an effectively zero level everywhere at $\alpha = 90°$.

In the heat transfer module in COMSOL, the above power dissipation is set as the thermal source, and the boundary of the region is set as a fixed temperature condition to simulate the normal tissue temperature. The thermal conductivity of the cell is set as approximately

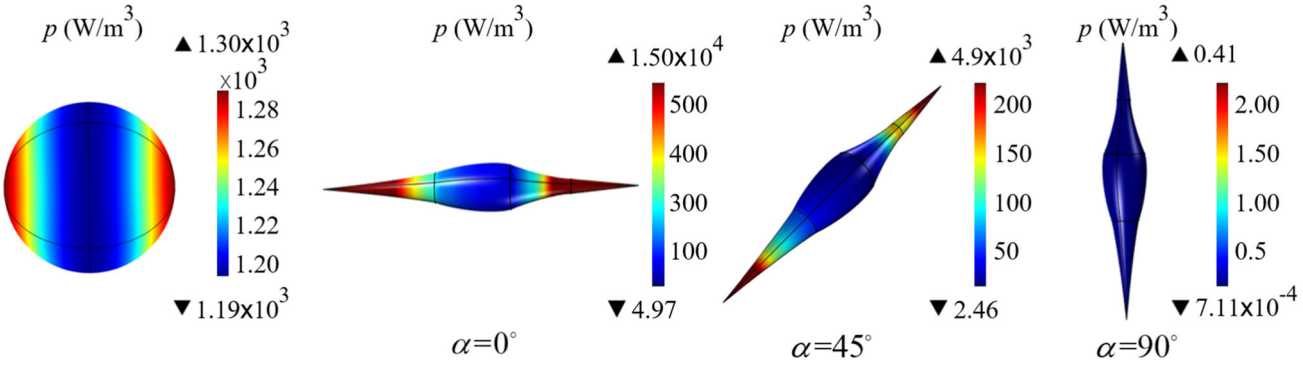

Fig. 7. The electromagnetic power dissipation distribution in the single-cell models.

0.6 W/m/K [Kyoo Park et al., 2013], and the initial and ambient temperature in and around the cell are set to 310.15 K (37°C), equal to the normal body temperature. The simulation results of the temperature rise in the single cell are shown in Figure 8.

Figure 8 shows that in the spherical model, the temperature distribution is almost uniform, but in contrast is highly variable in the irregular cell. To avoid the artifacts of discretization on the tips of irregular cell model, we calculated the average temperature rise over the whole-cell model to evaluate the thermal effect of TTFields. After calculation, the temperature rise in the spherical and irregular model is about 0.001 and 0.003 K, respectively. Thus, in both the spherical and irregular cell models, the thermal effect is observed to be very slight, due to the low intensity of the external electric field, even when the irregular shape is aligned directly with the field (the $\alpha = 0°$ case).

In order to verify the correctness of the thermal field simulation, we used an infrared camera to photograph the temperature distribution of cell culture medium with and without imposing an electric field. According to the microscopic image (not shown here), the HeLa cell has a similar shape as the U-87 cell, so we used HeLa cell culture to do the test. In the experiment, 2 ml of HeLa cell culture with the cell density 5×10^5 cells/ml was placed in two 35 mm diameter Petri dishes (Fisher Scientific, Pittsburgh, PA), one of which was fitted with electrodes to create a 2 V/cm, 200 kHz electric field using a Tektronix AFG 3120 function generator (Tektronix, Beaverton, OR). The two 20 mm × 10 mm cooper film electrodes (Bertech, Torrance, CA) are attached with adhesive to conform to the curved exterior dish wall. Exposure was kept for 10 min in order to reach a steady-state (room temperature, 24.8°C). The infrared camera (FLIR, Wilsonville, OR) was then used to photograph the Petri dishes (resolution, 0.1°C), and the images are shown in Figure 9. These figures show that the temperature distribution is not detectably different in the two cases, further suggesting that the power dissipation will not lead to a significant temperature rise and the thermal effect is unlikely to damage cell proliferation. It should be noted that we detected the temperature of the whole-cell culture, but not a single cell due to the technique's limitation. Nevertheless, this can still be validation on the thermal effect evaluation.

Frequency-Dependent Characteristics of Physical Fields. It is well-known [Goldman, 1943] from the capacitive nature of the cell membrane that its impedance decreases with increasing frequency.

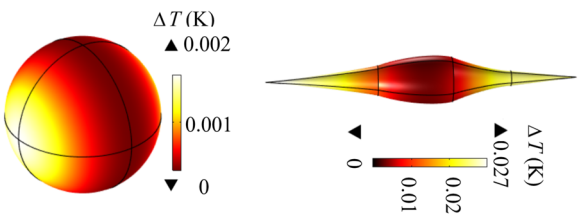

Fig. 8. The temperature rise of the single cell (only $\alpha = 0°$ in the irregular model is presented).

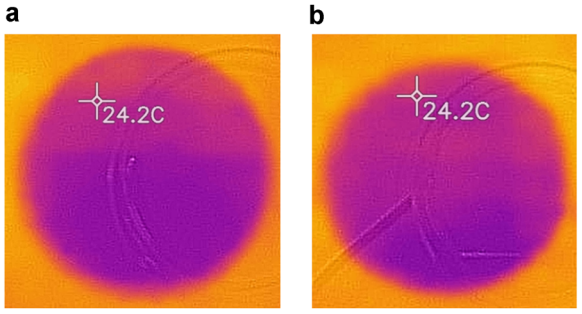

Fig. 9. The temperature distributions of HeLa cell culture: (**A**) without electric field; (**B**) with electric field.

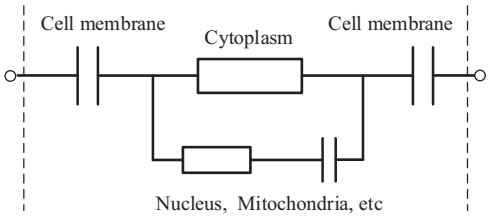

Fig. 10. The circuit model of the single cell.

An approximate circuit model of single cell is sketched in Figure 10. To address the frequency-dependent characteristics of electric fields and thermal effect in the single cell, the frequencies were varied from 100 kHz to 1 MHz, and the electrical properties of the cell are those used at 200 kHz because they are frequency-independent below 1 MHz. To reduce the distortion of FEM discretization, the average values of electric field intensity and temperature rise over the entire cell are demonstrated by curves in Figure 11A and B.

From these results in Figure 11, it can be seen that as the frequency increases, the electric field in the cell cytoplasm increases accordingly. It also shows that the ability of the electric field to penetrate the cell membrane becomes stronger, consistent with the circuit theory. While this increase is not linear, the electric field tends to be stable as the frequency climbs above 1 MHz. Additionally, even though the temperature in the cell has a slight rise (below 0.01 K in all cases), temperature changes less than about 0.1 K would be undetectable if the sensitivity of temperature measurement device is less than 0.1 K, and temperature changes within a cell, while not directly measurable, are calculated to be small with respect to normally occurring variations.

DISCUSSION

The response of biological cells to external electric fields is an interesting and important topic that requires insights from studies in biology and physics. Different electric field intensities and frequencies will cause different biophysical effects within the cell, and may have different medical implications. This paper focuses on the low-intensity, intermediate-frequency TTFields and studies their relevant electromagnetic field effects, with special emphasis on the electric field distribution and thermal effect.

As biological cells frequently assume an irregular shape, the electric field within the cell varies over a large range, leading to significant differences in exposure at cellular and sub-cellular dimensions. Noting that cells of tissues studied in vitro and in vivo are adherent, their cell shapes are much different from regular spheres, so the significant edge effect of the physical field distribution will be observed, as shown in the results section. Therefore, numerical algorithms incorporating more morphologically accurate cell geometries are recommended to improve accuracy.

When the cell is subjected to the TTField, the direction of the external electric field is an important factor affecting the electric field distribution in the cell. The highest electric field intensity will concentrate on the two ends of the cell when it is parallel to the direction of the external electric field. Consequently, electric field direction may enhance or diminish effects on cells and should be taken into consideration for medical devices and in research.

Thermal effects are one of the most essential biophysical mechanisms of electric fields in medical applications. For the nominal 2 V/cm intensity of the external electric TTField, the electric field within a

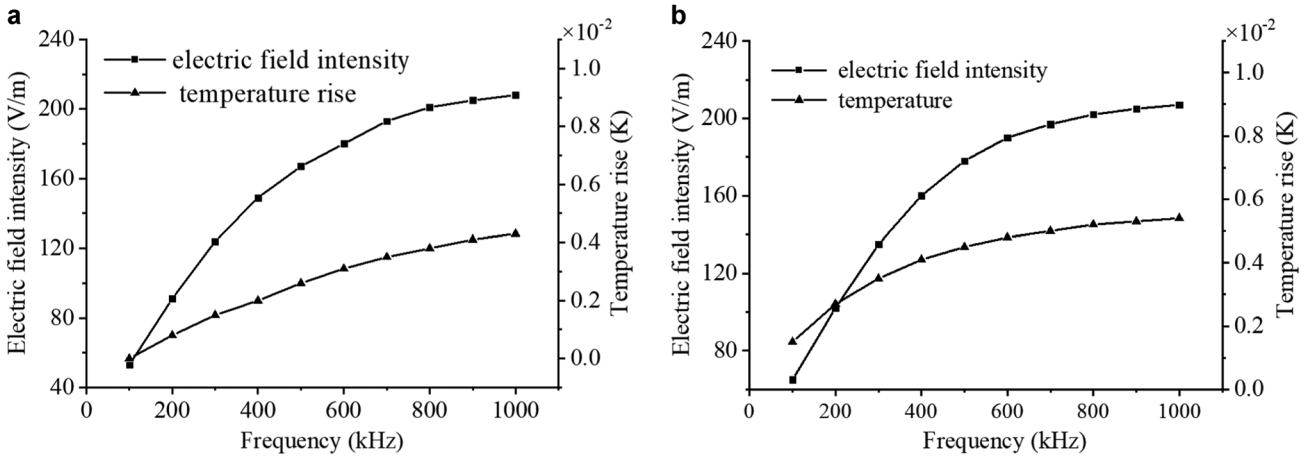

Fig. 11. The average electric field intensity and temperature change with the frequency increase: (**A**) the spherical model; (**B**) the irregular model.

cell corresponds to such low power dissipation that the rise in temperature is inconsequential and particularly is too small for thermal damage to a cell.

When the cell is exposed to an external alternating electric field, the cell membrane will act as a capacitor and shield the external electric field from entering the cell. For static and low frequency fields, the electric field in the membrane can be 10^5 greater than in the cytoplasm, but with increasing frequency membrane, capacitive impedance decreases and the cytoplasm electric field increases. But this frequency-dependent characteristic is not linear, and the electric field will tend to be stable when the frequency is over 1 MHz because the capacitive reactance becomes extremely small and the resistance component becomes dominant.

CONCLUSION

This work studied the electromagnetic and thermal effects of TTFields on a single cell. Spherical and irregular single-cell models have been used for numerical analysis. The results show that the distributions of electric field and temperature field in the spherical model are nearly uniform, whereas much greater field strengths occur at both ends of the irregular cell model. The electric field in the irregular cell depends heavily on its degree of alignment with the TTField; the more parallel the cell is to the TTField, the stronger electric field in the cell will be. Thermal effects in both cell models are not significant at the sub-cellular and cellular scales because electric fields coupled to the cell are too weak to cause detectable power loss. Thermographic evidence for an entire cell culture dish surface confirms the absence of a detectable temperature increase under the test conditions. Therefore, thermal effects can be excluded as a mechanism of observed clinical effects of TTFields. In our future work, the effects of the TTFields on dividing irregular cell will be studied and corresponding experiments will be conducted.

AUTHORS' CONTRIBUTIONS

Xing Li and Fan Yang developed the single-cell models and carried out the theoretical calculations. Bing Gao and Xiao Yu studied the simulations. Xing Li analyzed the results and drafted the manuscript. Boris Rubinsky gave some suggestions to the manuscript and improved it.

REFERENCES

Bottomley PA, Andrew ER. 1978. RF magnetic field penetration, phase shift and power dissipation in biological tissue: Implications for NMR imaging. Phys Med Biol 23: 630–643.

Büchner R, Hefter GT, May PM. 1999. Dielectric relaxation of aqueous NaCl solutions. J Phys Chem A 103:1–9.

Gascoyne PRC, Pethig R, Burt JPH, Becker FF. 1993. Membrane changes accompanying the induced differentiation of Friend murine erythroleukemia cells studied by dielectrophoresis. Biochim Biophys Acta 1146:119–126.

Gera N, Yang A, Holtzman TS, Lee SX, Wong ET, Swanson KD. 2015. Tumor treating fields perturb the localization of septins and cause aberrant mitotic exit. PLoS One 10:e0125269.

Giladi M, Schneiderman RS, Voloshin T, Porat Y, Munster M, Blat R, Sherbo S, Bomzon Z, Urman N, Itzhaki A, Cahal S, Shteingauz A, Chaudhry A, Kirson ED, Weinberg U, Palti Y. 2015. Mitotic spindle disruption by alternating electric fields leads to improper chromosome segregation and mitotic catastrophe in cancer cells. Sci Rep 5:18046.

Goldman DE. 1943. Potential, impedance, and rectification in membranes. J Gen Physiol 27:37–60.

Harris CM, Kell DB. 1983. The radio-frequency dielectric properties of yeast cells measured with a rapid, automated, frequency-domain dielectric spectrometer. Bioelectrochem Bioenerg 11:15–28.

Joshi RP, Hu Q, Schoenbach KH. 2004. Modeling studies of cell response to ultrashort, high-intensity electric fields—Implications for intracellular manipulation. IEEE Trans Plasma Sci 32:1677–1686.

Kirson ED, Dbalý V, TovaryŠ F, Vymazal J, Soustiel JF, Itzhaki A, Mordechovich D, Steinberg-Shapira S, Gurvich Z, Schneiderman R, Wasserman Y, Salzberg M, Ryffel B, Goldsher D, Dekel E, Palti Y. 2007. Alternating electric fields arrest cell proliferation in animal tumor models and human brain tumors. Proc Natl Acad Sci U S A 104:10152–10157.

Kirson ED, Gurvich Z, Schneiderman R, Dekel E, Itzhaki A, Wasserman Y, Schatzberger R, Palti Y. 2004. Disruption of cancer cell replication by alternating electric fields. Cancer Res 64:3288–3295.

Kotnik T, Miklavčič D. 2000a. Second-order model of membrane electric field induced by alternating external electric fields. IEEE Trans Biomed Eng 47:1074–1081.

Kotnik T, Miklavčič D. 2000b. Theoretical evaluation of the distributed power dissipation in biological cells exposed to electric field. Bioelectromagnetics 21:385–394.

Kyoo Park B, Yi N, Park J, Kim D. 2013. Thermal conductivity of single biological cells and relation with cell viability. Appl Phys Lett 102:3597–3599.

Mun EJ, Babiker HM, Weinberg U, Kirson ED, Von Hoff DD. 2018. Tumor treating fields: A fourth modality in cancer treatment. Clin Cancer Res 24:266–275.

Piacentini N, Mernier G, Tornay R, Renaud P. 2011. Separation of platelets from other blood cells in continuous-flow by dielectrophoresis field-flow-fractionation. Biomicrofluidics 5:034122.

Pless M, Droege C, Moos RV, Salzberg M, Betticher D. 2013. A phase I/II trial of tumor treating fields (TTFields) therapy in combination with pemetrexed for advanced non-small cell lung cancer. Lung Cancer 81:445–450.

Ponne CT, Bartels PV. 1995. Interaction of electromagnetic energy with biological material—Relation to food processing. Radiat Phys Chem 45:297–299.

Rehman AA, Elmore KB, Mattei TA. 2015. The effects of alternating electric fields in glioblastoma: Current evidence on therapeutic mechanisms and clinical outcomes. Neurosurg Focus 38:E14.

Schwan HP. 1957. Electrical properties of tissue and cell suspensions. Adv Biol Med Phys 5:147–209.

Sunderman FW. 1945. Measurement of serum total base. Am J Clin Path 15:219–222.

Turner SG, Gergel T, Wu H, Lacroix M, Toms SA. 2014. The effect of field strength on glioblastoma multiforme response in patients treated with the NovoTTF™-100A system. World J Surg Oncol 12:162.

Wenger C, Miranda PC, Salvador R, Thielscher A, Bomzon Z, Giladi M, Mrugala MM, Korshoej AR. 2018. A review on tumor treating fields (TTFields): Clinical implications inferred from computational modeling. IEEE Rev Biomed Eng 11:195–207.